Harnessing *Boerhavia diffusa's* Phytocompounds to combat Cisplatin - induced Renal Damage: Insights from Systems Pharmacology Analysis

Soora Sudarsanan Priyadharshini[1]*, Jaya Kumar Arun Kumar[1], Hari Rajeswary[1] and Rajendran Kowsalya[2]
1. Department of Biotechnology, Dr. M.G.R. Educational and Research Institute, Maduravoyal, Chennai- 600095, Tamil Nadu, INDIA
2. Department of Research, Meenakshi Academy of Higher Education and Research (MAHER), Chennai, 600078, Tamil Nadu, INDIA
*mail2priyamail@gmail.com

Abstract

Cisplatin-induced nephrotoxicity (DIN) restricts the clinical utility of this frontline chemotherapeutic, creating an urgent need for nephroprotective agents. Boerhavia diffusa (Punarnava) is a reputed drug for renal benefits in traditional medicine, but its molecular potential in drug induced nephrotoxicity DIN is yet to be elucidated. Chloroform and ethanol extracts of Boerhavia diffusa leaves underwent GC-MS profiling, revealing 40 phyto compounds (26 chloroform, 14 ethanol). Drug-likeness and specificity were evaluated using Swiss ADME, narrowing the list to 20 compounds. Network pharmacology mapped these phytoconstituents to 80 genes implicated in cisplatin nephrotoxicity, identifying six key hub proteins: AKT1, AMPK, BCL2, CASP3, NLRP3 and OCT, enriched in apoptotic, pyroptotic and drug transport pathways (FDR < 1 × 10^{-36}). Auto Dock Vina-based molecular docking screened all actives against these targets and top interactions were structurally characterized.

Five leads (DHP, HMPFP, BTDMP, Methylenebis, Flavone) displayed high binding affinities (≤ –10.5 kcal/mol) to multiple targets. DHP and HMPFP exhibited robust hydrogen bonding and π-stacking within AKT1 and NLRP3 pockets, blocking key sites (e.g. Gln179, Trp80, Arg298) and impeding ATP access. BTDMP further bridged AKT1 and plugged NLRP3 and OCT channels. These multi-target interactions indicate modulation of autophagy (via AKT1/AMPK), attenuation of inflammasome-driven pyroptosis (NLRP3) and inhibition of cisplatin uptake (OCT). DHP, HMPFP and BTDMP from B. diffusa emerge as orally bioavailable, multi-target nephroprotective candidates, meriting further in vivo validation against cisplatin nephrotoxicity.

Keywords: Drug induced nephrotoxicity, Cisplatin, *Boerhavia diffusa*, Apoptosis, Drug transport, Molecular mechanisms.

Introduction

Drug-induced nephrotoxicity, especially from widely used chemotherapeutic agent like cisplatin, remains a critical barrier in clinical practice, underscoring the need for novel nephroprotective strategies with minimal adverse effects. Nephrotoxicity arises through a multifaceted cascade involving oxidative stress, mitochondrial dysfunction, inflammation, fibrosis and apoptosis, complications further aggravated by various drugs including antibiotics, nonsteroidal anti-inflammatory drugs (NSAIDs) and cytotoxins[28].

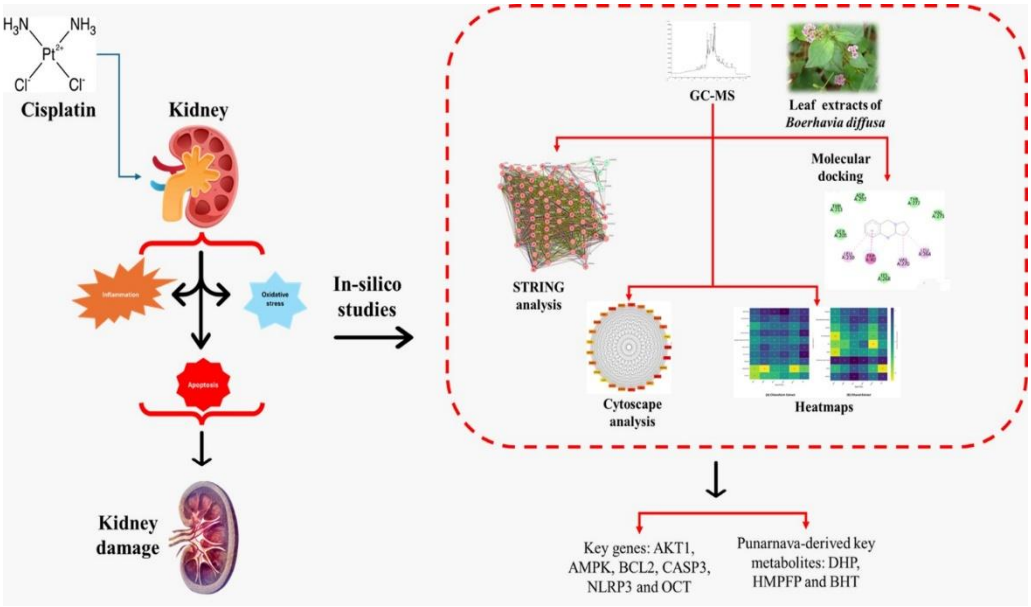

Graphical Abstract

Despite the critical need for effective renal protection in patients dependent on these agents or chronic disease management, current therapeutic strategies often prove inadequate in preventing or reversing nephrotoxic injury. This therapeutic gap has spurred growing scientific interest in plant-based alternatives possessing multi-modal bioactivities, with the potential complement or replacing nephroprotective agents[37]. Phytochemicals, owing to their structural diversity and broad spectrum of biological activities, have shown significant potential in ameliorating renal injury by modulating key molecular pathways linked to kidney damage.

Plant-derived metabolites, especially those with antioxidant, anti-inflammatory and anti-apoptotic properties, provide a rational foundation for developing new anti-nephrotoxic interventions, merging traditional medicinal wisdom with contemporary biomedical research[10,22]. *Boerhavia diffusa* (Punarnava), a staple plant in Ayurveda and other traditional systems, is reputed for its efficacy in treating kidney and liver disorders, as well as edema[34]. These therapeutic effects are attributed to its rich profile of alkaloids, flavonoids, terpenoids, phenolics and glycosides. However, while anecdotal and historical evidence abound there is a marked paucity of rigorous, mechanistic studies using modern analytical methods to validate its role in drug-induced nephrotoxicity[2,25].

Thus, this raises a question; can specific bioactive compounds isolated from *B. diffusa* provide nephroprotective effects against cisplatin-induced renal injury, as predicted by contemporary in silico approaches?

To address this, the present study integrates investigative techniques including GC-MS-based phytochemical profiling, *in silico* pharmacokinetic studies (ADME - absorption, distribution, metabolism and excretion), molecular docking and systems-level network pharmacology, to identify and characterize the interactions between *B. diffusa*-derived phytoconstituents and renal molecular targets implicated in cisplatin nephrotoxicity. By mapping the involvement of key proteins such as AKT1, AMPK, BCL2, CASP3, NLRP3 and OCT2, each pivotal to cell survival, inflammation, apoptosis and drug transport, this comprehensive approach seeks to predict the nephroprotective efficacy and mechanistic action of Punarnava's bio actives[18,19,21,26,35]. Collectively, this strategy aims to fill critical knowledge gaps and to guide the development of effective, plant-based therapies for drug-induced renal injury.

Material and Methods

Sample Collection: The *Boerhavia diffusa* plant samples were procured from the Arignar Anna Government Hospital of Indian Medicine, Arumbakkam, Chennai, Tamil Nadu, India. These samples were selected for their traditional medicinal uses and were processed immediately after collection to maintain the integrity of bioactive compounds.

Sample Preparation: The collected leaves were thoroughly washed with distilled water to remove any external contaminants such as mud, dust and debris. Subsequently, the leaves were air-dried in the shade for a period of 7–10 days to prevent degradation of heat-sensitive bioactive compounds. Once dried, the leaves were finely ground into powder using either a motor and pestle or an electric grinder.

Extraction: A cold maceration method was employed to extract bioactive compounds. Ten grams of the powdered leaf material was soaked in 100 mL of chloroform and ethanol respectively (1:10 w/v ratio) for 72 hours at room temperature, with continuous shaking at minimal speed in a rotary incubator. After the incubation period, the mixture was filtered through Whatmann no. 1 filter paper to obtain the chloroform and ethanolic extracts respectively. The filtrate was then concentrated using a rotary evaporator set at 40ºC to remove the solvent. The dry extract was weighed after complete evaporation of the solvent and the yield percentage was calculated using the following formula[23]:

Yield % = (Weight of the extract / Weight of the plant material) * 100.

GC-MS Analysis: The phytochemical profile of the *Boerhavia diffusa* leaf extract was analyzed using a GC-MS-QP2010 Plus instrument. The initial oven temperature was set at 50°C for 2 minutes followed by a temperature ramp to 280°C at a rate of 10°C/min and a final hold for 5-10 minutes at 280°C. 1 µL injection was used with a split ratio of 10:1 and helium gas was used as the carrier at a flow rate of 1 mL/min. The mass spectra of the eluted compounds were compared to the NIST and Wiley spectral libraries for compound identification.

Drug-likeness Analysis: The drug-likeness and pharmacokinetic properties of the bioactive compounds identified in the *Boerhavia diffusa* extract were predicted using the Swiss ADME online tool (http://www.swissadme.ch/). The Simplified Molecular Line Entry System (SMILES) notation for each identified compound was input into the tool to predict various ADME (Absorption, Distribution, Metabolism and Excretion) properties[4].

Gene Identification: To explore the molecular mechanisms underlying cisplatin-induced nephrotoxicity, relevant genes were identified using the Gene Cards database (https://www.genecards.org/) and the Comparative Toxicogenomics Database (CTD) (https://www.ctdbase.org/). The search was conducted using keywords such as "Cisplatin Nephrotoxicity," "Cisplatin induced acute renal injury," and "Cisplatin induced chronic renal failure"[15,39].

Additionally, a comprehensive literature review of cisplatin-induced nephrotoxicity was performed to cross-verify the findings[6,36]. A total of 80 genes implicated in cisplatin nephrotoxicity were selected for further analysis.

Protein–Protein Interaction Network: The identified genes were used to construct a protein–protein interaction (PPI) network using the STRING database (https://string-db.org/), a reliable tool for visualizing functional associations and interactions between proteins[29]. The "Homo sapiens" organism was selected and a medium confidence score (0.4) was applied to filter the interactions. Subsequently, gene ontology (GO) enrichment and Kyoto Encyclopedia of Genes and Genomes (KEGG) pathway analyses were performed to identify key biological processes and molecular pathways involved in cisplatin nephrotoxicity.

Pathways and Functional Enrichment Analysis: The molecular pathways and functional enrichment of the identified genes were further analyzed using the ShinyGo 0.81 database (https://bioinformatics.sdstate.edu/go/). This tool provides insights into gene functional categorization and helps in understanding the molecular pathways involved in cisplatin-induced nephrotoxicity[8].

Molecular Docking: The bioactive compounds identified through GC-MS analysis were subjected to molecular docking to assess their binding affinity with key proteins associated with cisplatin nephrotoxicity. SMILES notation for each compound was retrieved from PubChem (https://pubchem.ncbi.nlm.nih.gov/) and PDB (Protein Data Bank) structures were generated using the CACTUS tool (https://cactus.nci.nih.gov/translate/). Protein structures for 20 key nephrotoxic proteins were downloaded from the Protein Data Bank (https://www.rcsb.org/) and prepared for docking by removing water molecules and unwanted ligands using the Discovery Studio software. The docking simulations were carried out using PyRx, an open-source molecular docking tool, to evaluate the binding affinity and interaction of the plant compounds with their target proteins[5].

Results and Discussion

Extraction Yield: The extraction yield from *B. diffusa* leaves varied significantly depending on solvent polarity, reflecting the diversity of compounds solvated by each solvent type. The ethanol extract yielded a comparatively higher yield of 2.15% compared to 1.37% from the chloroform extraction.

GC-MS Analysis: The GC-MS profiling of chloroform and ethanol extracts of *B. diffusa* unveiled distinct yet complementary phytochemical profiles. Chloroform extract analysis (Table 1, Figure 1a) yielded 26 metabolites, prominently oleic acid (45.32% area) and n-hexadecanoic acid (20.89% area). The ethanol extract (Table 2, Figure 1b) contained 14 metabolites, notably eicosatrienoic acid (20.97%), phytol (16.77%) and hexadecanoic acid ethyl ester (10.48%).

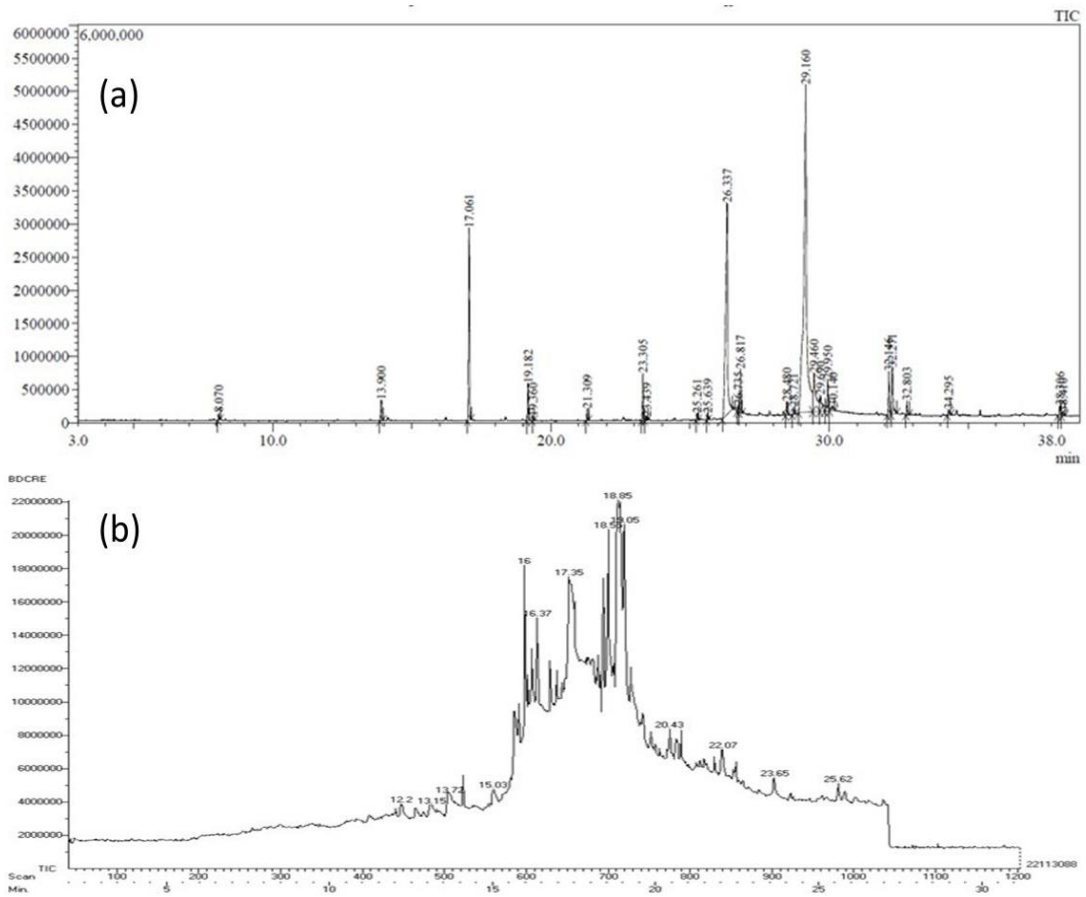

Figure 1: GCMS chromatogram of *Boerhavia diffusa* a) Chloroform Extract (BDCE) b) Ethanol Extract (BDEE)

Table 1
GCMS compounds identified *Boerhavia diffusa* Chloroform Extract (BDCE)

Peak	Retention Time	Ligands	Molecular Formula	Molecular Weight g/mol	Area %
1	8.07	1-Dodecanol	$C_{12}H_{26}O$	186.33	0.29
2	13.9	1-Tetradecanol	$C_{14}H_{30}O$	214.39	0.01
3	17.061	2,4-Di-tert-butylphenol	$C_{14}H_{22}O$	206.32	8.87
4	19.182	1-Nonadecene	$C_{19}H_{38}$	266.5	1.62
5	19.36	Heptadecane	$C_{17}H_{36}$	240.5	0.15
6	21.309	Dodecylacrylate	$C_{15}H_{28}O_2$	240.38	0.5
7	23.305	1-Nonadecene	$C_{19}H_{38}$	266.5	1.94
8	23.439	Heptadecane	$C_{17}H_{36}$	240.5	0.15
9	25.261	7,8-Di-tert-butyl-I-oxaspiro(48)deca-6,9-diene-2,8-dione	$C_{17}H_{24}O_3$	276.37	0.29
10	25.639	Hexadecanoicacid, methyl ester	$C_{17}H_{24}O_2$	270.45	0.28
11	26.337	n-Hexadecanoic acid	$C_{16}H_{32}O_2$	256.42	20.89
12	26.735	1,4-benzenediol,2,5-bis(1,1-dimethylpropyl)-	$C_{16}H_{26}O_2$	250.38	0.29
13	26.817	1-Nonadecene	$C_{19}H_{38}$	266.5	1.9
14	28.48	9-octadecenoicacid(z)-, methyl ester	$C_{19}H_{36}O_2$	296.49	0.6
15	28.721	4H-1-Benopyran-6-Carboxaldehy	$C_{10}H_6O_3$	174.15	0.35
16	29.16	Oleic Acid	$C_{18}H_{34}O_2$	282.5	45.32
17	29.46	Octadecanoic acid	$C_{18}H_{36}O_2$	284.5	4.98
18	29.69	Hexadecanamide	$C_{16}H_{33}NO$	255.44	1.71
19	29.95	1-Hexacosanol	$C_{26}H_{54}O$	382.7	1.91
20	30.14	1-Docosanol,acetate	$C_{24}H_{48}O_2$	368.6	0.46
21	30.14	3,3,5,5'-Tetra-tert-butylbiphenyl-2,2-diol	$C_{28}H_{42}O_2$	410.6	2.09
22	32.271	9-Octadecenamide, (Z)-	$C_{18}H_{35}NO$	281.5	2.64
23	32.803	1-Hexacosanol	$C_{26}H_{54}O$	382.7	0.58
24	34.295	Hexadecanoic Acid, 2-Hydroxy-1-(Hydroxymethyl)Ethyl Ester	$C_{19}H_{38}O_4$	330.5	0.3
25	38.306	1H-Isoindole-1,3(2H)-dione, 2,2'-methylenebis-	$C_{17}H_{10}N_2O_4$	306.27	0.62
26	38.41	Squalene	$C_{30}H_{50}$	410.7	0.25

Pharmacokinetics Analysis: GC-MS profiling and pharmacokinetic analysis effectively identified diverse bioactive metabolites capable of interfering with these critical pathways. Pharmacokinetic screening refined the identified metabolites, isolating 20 candidates (10 from each extract) that satisfied critical drug-likeness criteria such as Lipinski's Rule of Five, Ghose, Veber, Egan and Muegge parameters (Table 3). Notably, most selected compounds elicited minimal or no Pan-Assay Interference Compound (PAINS) alerts, affirming their reliability as therapeutic leads. Specifically, compounds such as DHP, HMPFP, BTDMP, Methylenebis and Flavone demonstrated excellent pharmacokinetic profiles including favorable absorption, distribution, metabolism and excretion characteristics, essential for bioavailability and minimal side effects.

Network Pharmacology: Network pharmacology analysis identified AKT1(alpha serine/threonine-protein kinase), AMPK (AMP-activated protein kinase), BCL2(B-cell lymphoma 2), CASP3(Cysteine-aspartic acid protease 3), NLRP3(NOD-like receptor family, pyrin domain) and OCT2 (Organic Cation Transporter 2) as pivotal hub proteins implicated in cisplatin-induced nephrotoxicity (Figure 2). AKT1, BCL2 and CASP3 are central regulators of apoptosis, significantly influencing renal cell survival and death during cisplatin treatment. AMPK and NLRP3 represent critical nodes in metabolic stress and inflammasome-mediated inflammatory pathways. OCT2 prominently mediates cisplatin renal uptake, significantly contributing to nephrotoxicity[7,16,17,31].

The protein–protein interaction network generated from STRING and Cytoscape, highlighted significant enrichment of pathways involving apoptosis, oxidative stress response, inflammasome activation and organic ion transport. GO and KEGG pathway analyses notably identified apoptosis and platinum drug resistance pathways among the significantly enriched pathways (Figure 2c).

Table 2
GCMS compounds identified *Boerhavia diffusa* Ethanol Extract (BDEE)

Peak	Retention Time	Ligands	Molecular Formula	Molecular Weight (g/mol)	Area %
1	12.2	2H-1-Benopyran,3,5,8,8a-tetrahydro_2,5,5,8a-tetramethyl-	$C_{14}H_{22}O$	206.32	1.05
2	13.15	a-Ylangene	$C_{15}H_{24}$	204.35	1.68
3	13.72	1H-Imidazole,4,5-dihydro-2-(1,2,3,4-tetrahydro-1-naphthalenyl)-	$C_{13}H_{17}ClN_2$	236.74	2.05
4	15.03	Flavone	$C_{15}H_{10}O_2$	222.24	2.52
5	16	11-Tetradecyn-1-ol acetate	$C_{16}H_{28}O_2$	252.39	12.58
6	16.37	17H-Cyclopenta(a)phenanthren-17-one,11,12,13,16-tetrahydro-3-methoxy-13_methyl-,(S)-	$C_{19}H_{20}O_2$	280.36	8.39
7	17.35	Hexadecanoicacid,ethyl ester	$C_{18}H_{36}O_2$	284.5	10.48
8	18.58	Phytol	$C_{20}H_{40}O$	296.5	16.77
9	18.85	B,11,14,Eicosatrienoic acid(Z,Z,Z)-	$C_{20}H_{34}O_2$	306.28	20.97
10	19.05	Octadecanoic acid,3-oxo-,methyl ester	$C_{19}H_{36}O_3$	312.5	14.68
11	20.43	15-Isopropenyl-3-(trimethylsilyl)oxacyclopentadecan-2-one	$C_{19}H_{36}O_2Si$	338.6	4.19
12	22.07	1H-Pyrrolo[2,3-b]quinoxaline_2-imine,2,3,3ª,4,9,9ª-hexahydro-1,N-diphenyl-	$C_{24}H_{23}N_3$	340.44	3.14
13	23.65	{5-(3-Hyroxy-3-methyl-but-1-ynyl}-furan-2-yl]-[4-{4-methoxy-phenyl}-piperazin-1-yl]-methanone	$C_{25}H_{28}N_2O_4$	398.48	2.1
14	25.62	Phenol,2,6,bis(1,1-dimethylethyl)-4-[{4-hydroxy-3,5-dimethylphenyl}methyl]-	$C_{23}H_{32}O_2$	340.5	1.17

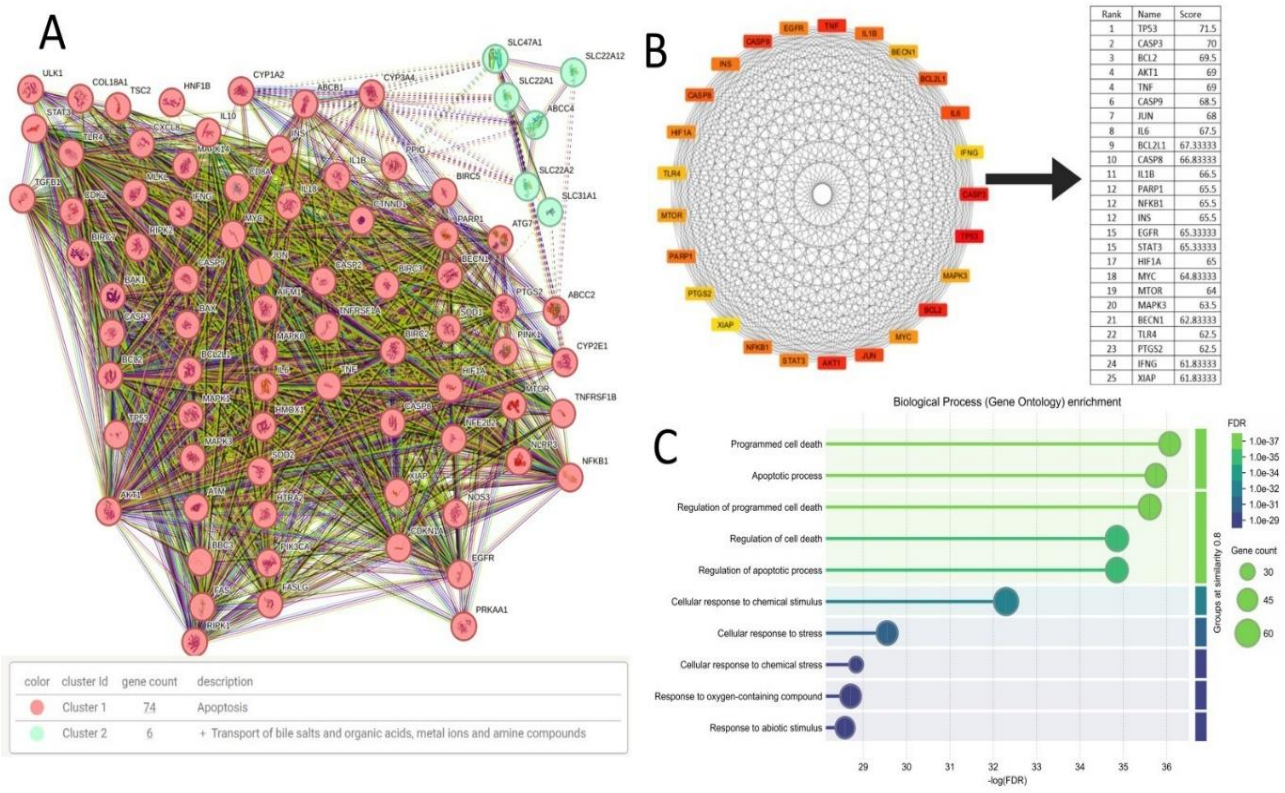

Figure 2: Network Pharmacology studies
(a) Cisplatin Nephrotoxic gene interaction network represented as two clusters obtained from the STRING database based on target cluster. (b) Top 25 rank protein - protein interaction from Cytoscape (c) Gene Ontology studies

Table 3
Pharmacokinetic Analysis – Short listed Compounds from Chloroform and Ethanol Extract

S.N.	Ligand Name	Common Name/Short name	Druglikeness evaluation – No. of violation for each rule					Pains alerts
			Lipinski	Ghose	Veber	Egan	Muegge	
***Boerhavia diffusa* Chloroform Extract (BDCE)**								
1	1-Dodecanol	Dodecanol	0	0	0	0	2	0
2	1-Tetradecanol	Tetradecanol	0	0	1	0	2	0
3	2,4-Di-tert-butylphenol	DTBP	0	0	1	0	2	0
4	Hexadecanoicacid,methyl ester	Methyl Palmitate	1	0	1	0	1	0
5	1,4-Benzenediol,2,5-Bis(1,1-Dimethylpropyl)-	Butylated Hydroxyanisole BHA	0	0	0	0	1	0
6	9,Octadecenoicacid(z)-, methyl ester	Methyl Oleate	0	0	1	0	2	0
7	Hexadecanamide	Palmitamide	0	0	1	0	1	1
8	9-Octadecenamide, (Z)-	Oleamide	1	0	1	0	1	0
9	1H-Isoindole-1,3(2H)-dione, 2,2'-methylenebis-	Methylenebis	0	0	0	0	0	0
10	Squalene	Squalene	0	0	0	0	0	0
***Boerhavia diffusa* Ethanol Extract (BEEE)**								
11	Octadecanoic acid,3-oxo-, methyl ester	Octadecanoic acid	0	0	1	0	2	0
12	a-Ylangene	a-Ylangene	1	0	0	0	1	0
13	1H-Imidazole,4,5-dihydro-2-(1,2,3,4-tetrahydro-1-naphthalenyl)-	TNI - (Tetralinyl) imidazoline	0	0	0	0	0	0
14	17H-Cyclopenta(a)phenanthren-17-one,11,12,13,16-tetrahydro-3-methoxy-13_methyl-,(S)-	MMTHCP - Methoxy methyl tetra Hydro Cyclopenta Phenanthren	0	0	0	0	0	0
15	Phenol,2,6,bis(1,1-dimethylethyl)-4-[{4-hydroxy-3,5-dimethylphenyl}methyl]-	BTDMP - Bis-tert-butyl-dimethylpheylmethylphenol	0	0	0	0	0	0
16	1H-Pyrrolo[2,3-b]quinoxaline_2-imine,2,3,3ª,4,9,9ª-hexahydro-1,N-diphenyl-	DHP - Diphenyl-Hexahydro-Pyrroloquinoxaline.	0	0	0	0	0	0
17	{5-(3-Hyroxy-3-methyl-but-1-ynyl}-furan-2-yl]-[4-{4-methoxy-phenyl}-piperazin-1-yl]-methanone	HMPFP - Hydroxy Methyl Phenyl Furan Piperazine	0	0	0	0	0	1
18	2H-1-Benopyran,3,5,8,8a-tetrahydro_2,5,5,8a-tetramethyl-	TMBP –Tetramethyl-tetrahydrobenzopyrn	0	1	0	0	2	0
19	Flavone	Flavone	0	0	0	0	0	0
20	Acetamide, 2-(diethylamino)-n-(2,6-dimethylphenyl)-	Lidocaine	0	0	0	0	0	0

Thus, the network data provided molecular insight into the critical pathways disrupted by cisplatin, serving as robust biological targets for *Boerhavia diffusa* metabolites. The identified hub proteins: AKT1, AMPK, BCL2, CASP3, NLRP3 and OCT2, orchestrate an interconnected pathway crucial for the initiation and progression of cisplatin-induced kidney injury. It is understood that AKT1 and BCL2 inhibition exacerbates tubular apoptosis, whereas caspase-3 activation directly mediates cellular death[27,32,40]. AMPK, although protective in moderate activation, becomes deleterious when excessively stimulated by cisplatin, driving apoptosis via p53 activation[13,38]. Concurrently, NLRP3 inflammasome activation by oxidative stress signals triggers inflammatory cytokine release, further amplifying renal injury[28,31]. The cisplatin uptake is transporter-mediated, primarily via OCT2, accentuates intracellular platinum accumulation, intensifying nephrotoxic outcomes[3,14].

Docking Studies: Molecular docking was performed for *Boerhavia diffusa*-derived ligands to validate and extend the network findings with the six key protein targets. Figure 3 summarizes the binding affinity results as heatmaps for compounds from the chloroform extract (Figure 3a) and ethanol extract (Figure 3b). Five ligands: DHP, HMPFP, BTDMP, Methylenebis and Flavone, exhibited robust affinity toward multiple targets, indicative of their multi-modal nephroprotective potential (Figure 3 and table 4). The docking poses of the top three ligands (categorized based on the binding affinity score) with the target proteins are represented in figures 4 and 5.

AKT is a crucial enzyme involved in cell signalling pathways leading to apoptosis. Upon docking with AKT (Figure 4a), the top docked ligands bind deeply within the ATP-binding cleft of AKT. Notably, the phyto ligand BTDMP forms two hydrogen bonds with the hinge backbone of the AKT1 receptor at Gln79 and Thr82, mimicking the adenine ring of ATP. A salt-bridge/hydrogen-bond interaction is observed with Asp292 of the conserved DFG motif (activation loop), as shown by the orange dashed line. Hydrophobic contacts surround the ligand: for example, Trp80 (in the glycine-rich loop) packs against the ligand's aromatic ring system and Val270/ 271 and Tyr272 (in the kinase substrate pocket) provide a hydrophobic enclosure.

Recent research reported by Biswas et al[1], has demonstrated that the ligands withaferin A and garcinol when docked with AKT1 and BCL2 showed higher binding affinity of -11 kcal/Mol and -13kcal/Mol respectively, contributing to cellular protection, which aligns with our findings where the top three ligands exhibited the binding affinity to AKT1 at a range of -10.8 kcal/Mol to -9.5 kcal/Mol. Overall, the docking poses for AKT1 indicate that all three compounds can effectively mimic ATP or known kinase inhibitors by engaging the hinge via hydrogen bonding and filling the hydrophobic adenine-binding pocket.

In the present study, a similar interaction profile was observed for the AMP-activated protein kinase (AMPK) (Figure 4b). It is observed from the virtual studies that AMPK's catalytic α-subunit shares a homologous kinase domain to AKT1. Here the pyto ligands DHP and HMPFP again target the ATP-binding site.

On the other hand, Methylenebis, in particular, shows a strong electrostatic interaction with an active-site residue Arg which likely corresponds to the conserved Arg of the HRD motif in kinases. This salt bridge, together with hydrophobic contacts such as Val/Ile in the pocket binding to AMPK by the above phyto ligands, halts their action. More over the ligands such as DHP and HMPFP also form H-bonds with residues (Arg298) on AMPK's hinge/activation loop region. Methylenebis also engages Ser241 and Arg268, giving it three polar anchors, while burying hydrophobic rings against Val296, Ile239, Leu276, Phe272. The shared Arg 298 in HMPFP retains the Arg 298 contact but depends otherwise on hydrophobic enclosure by VAL296 and Leu276.

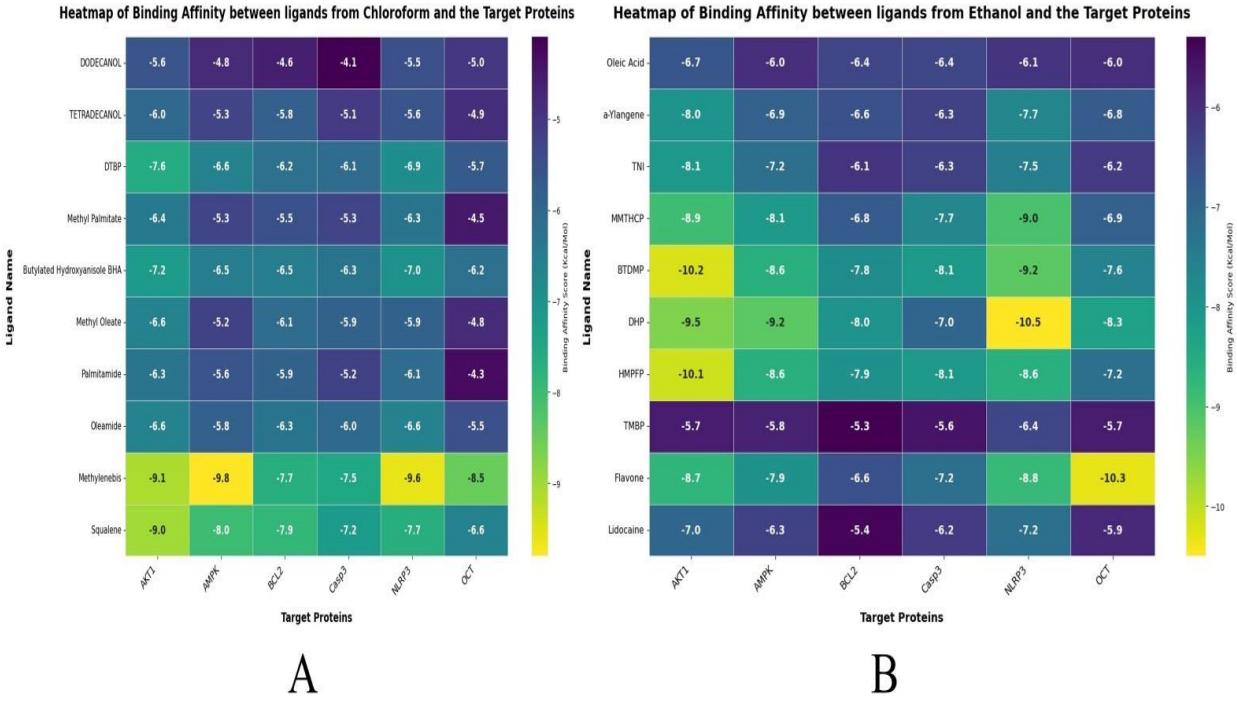

Figure 3: Binding affinity heatmap for *B. diffusa*-derived ligands from Chloroform and Ethanol Extract Docked against six nephrotoxicity-associated protein targets (AKT1, AMPK, BCL2, CASP3, NLRP3 and OCT). Lighter colors (green/yellow) indicate more negative binding energies (stronger affinities) whereas darker colors (blue) indicate weaker binding (scale bar in kcal/mol).

DHP restores an extensive hydrophobic network with Ile239, Val296, Leu276, Val275. In our study,1H-Isoindole-1,3(2H)-dione, 2,2'-methylenebis-(Methlenebis) exhibited the highest binding affinity to AMPK with binding affinity of -9.8Kcal/Mol, indicating strong interaction potential. Supporting this, recent research had reported that isoindolne-1,3-dione derivatives with specific functional modifications effectively activate AMPK[20].

BCL2 family proteins are key anti - apoptotic proteins that function either as inhibitors (BCL2) or activator (Bax). BCL2 preserves mitochondrial membrane integrity by locking cytochrome c release and caspase activation, thereby regulating apoptosis[33]. From figure 4 (c), it could be observed that the ligands interact with the elongated BH3-binding groove of the anti-apoptotic protein. This groove is lined by hydrophobic residues and a few polar hotspots. The docking results in the present study show DHP fits snugly into this groove, spanning the hydrophobic pocket formed by Tyr9, Trp195, Ile189 and Gln190 with π-stacking with Tyr9 and Trp195, while also forming key polar contacts.

HMPFP also forms hydrophobic π-stack interaction with TYR9 and THR7, while maintaining hydrogen bonds with common amino acid residues in the binding site. BTDMP adds a π-contact to His186 and keeps the Tyr9 / Trp195 interactions, marginally increasing surface contact. It is reported by Sharma et al[24], that baicalin, a bioactive compound, has strong and stable binding to BCl2 receptors (-9 kcal/Mol), supported by molecular docking and dynamic stimulations, that orient with our current findings, where the phyto ligands such as DHP, HMPFP and BTDMP demonstrated comparable binding affinities in the range of -8 to -7.8kcal/mol, thereby reinforcing their potential, a promising anti-apoptotic agent through similar molecular interactions[24].

When docked with Caspase-3 (Figure 5a), the compounds target the enzyme's substrate-binding cleft and catalytic site. Caspase-3 is a cysteine protease with a catalytic dyad. Strikingly, the docking poses show ligands situated near this active-site cleft: for example, BTDMP foregoes ionic contacts, forges two hydrogen bonds to Thr140 and Tyr195 BTDMP (green) while its ring system spans Lys137 and Pro201. HMPFP inserts into the cleft and interacts directly with the catalytic histidine (Arg164) via hydrogen bond or π–cation interaction (orange highlight).

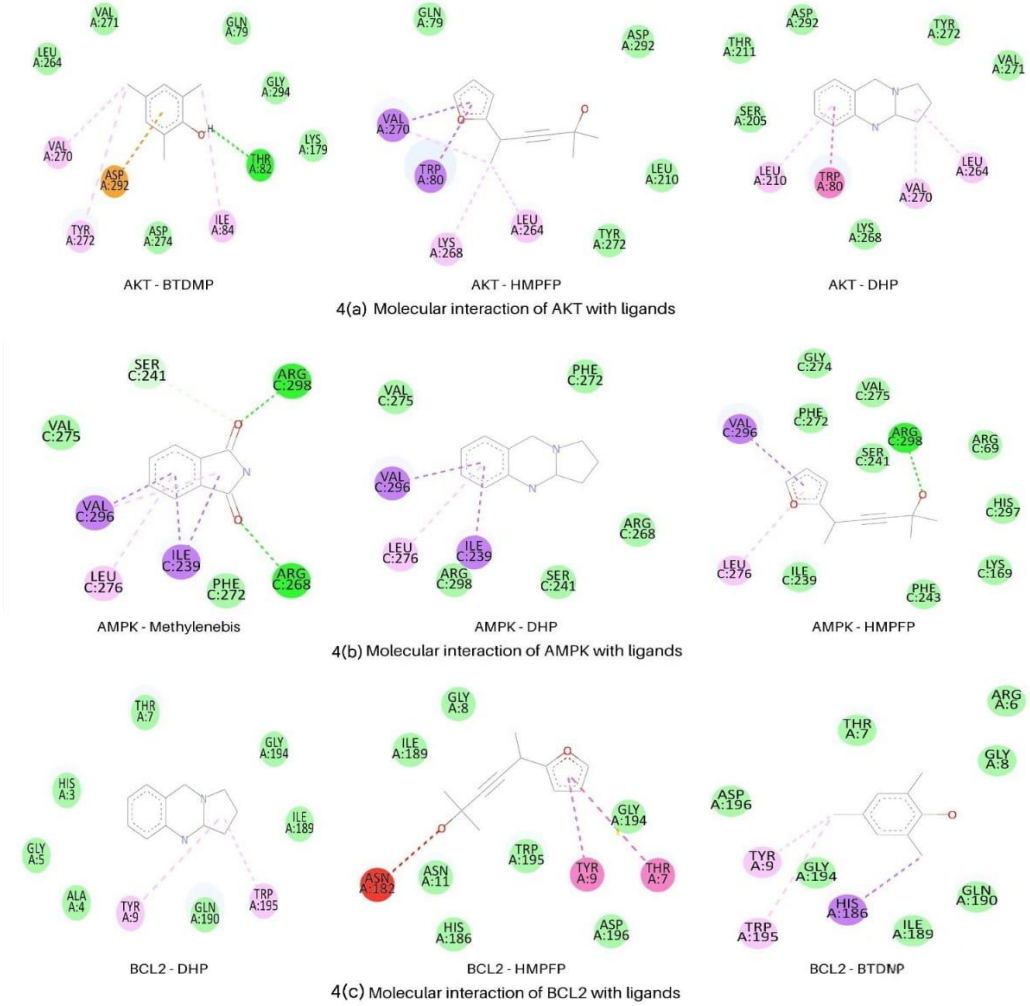

Figure 4: Molecular interactions of target proteins 4 (a) AKT, 4(b) AMPK and 4(c) BCL2 with top three interacting ligands

Table 4
Various types of interactions involved in ligand-target molecular docking analysis.

S.N.	Target protein	Ligand	Binding Affinity (Kcal/Mol)	Hydrogen -bond	Hydrophobic interaction
1.	AKT1	BTDMP	-10.2	Leu264, Val271, Gln79, Gly294, Lys179, Thr82, Asp274	Val270, Asp292, Tyr272, Ile84
		HMPFP	-10.1	Gln79, Asp292, Leu210, Tyr272	Val270, Trp80, Lys268, Leu264
		DHP	-9.5	Ser205, Thr211, Asp292, Tyr272, Val271, Lys268	Leu210, Trp80, Val270, Leu264
2.	AMPK	Methylenebis	-9.8	Arg298, Arg268, Phe272, Ser241, Val275	Val296, Ile239, Leu276
		DHP	-9.2	Arg298, Arg268, Phe272, Ser241, Val275	Val296, Ile239, Leu276
		HMPPF	-8.6	Arg298, Phe272, Val275, Ser241, Gly274, Arg69, His297, Lys169, Phe243, Ile239	Val296, Leu276
3.	BCL2	DHP	-8	Gly194, Ile189, Thr7, His3, Gly5, Ala4, Gln190	Tyr9, Trp195
		HMPFP	-7.9	Gly8, Gly194, Ile189, Asn11, His186, Trp195, AsP196	TyR9, Thr7
		BTDMP	-7.8	Gly8, Gly194, Ile189, Thr7, Gly8, Arg6, Gln190	Tyr9, TrP195, His186
4.	Casp3	BTDMP	-8.1	Gly125, Tyr197, Leu136, Thr140, Tyr195	Lys137, Pro201
		HMPFP	-8.1	Gly125, Lys137, Arg164, Gly202	Lys137, Pro201, Tyr197, Val266, Arg164
		Methylenebis	-7.5	Glu124	Arg164, Pro201, Tyr197, VaL266
5.	NLRP3	DHP	-10.5	Thr233, Ile521, Lys232, Gly231, Gly229	Ile234, His522, TrP416, Leu413
		Methylenebis	-9.6	Thr439, Arg578, Phe575, Ala227, Ala228, Gly229, Thr524, LeU413, Tyr443, VaL414, Met661, Met408	Ile411
		BTDMP	-9.2	Trp416, Gly231, Thr169, Tyr168, Arg167	Leu413, Pro412, Leu171, Ile234, Phe373
6.	OCT	Flavone	-10.3	Phe238, Ser239, Asp385, Gly442, Val441, Phe356	His242, Lys389, Cys32, Phe445, Phe360
		Methylenebis	-8.5	Gly209, Ala206, Trp175, Gln179, Ser176, Phe205	Ala159, Cys160, Ala163, Val172
		DHP	-8.3	Ala163,Gly156,Ala206,Ser176,Gln179	Val172,Cys160,Phe205,Ala159

Hydrogen-bonding to an adjacent Lys137 and Arg164 is making hydrophobic contacts with surrounding residues. All ligands nestle between the two catalytic chains and converge on the dual Arg164 residues that normally secure a substrate Asp. Methylenebis recreates a dual salt-bridge with ARG164 from both chains and adds π-stacking to Tyr197.

BTDMP, generated the tightest polar–hydrophobic clamp observed. Such a binding mode could competitively inhibit caspase-3 by occupying the active site and blocking access to the protein substrate. By stabilizing the catalytic pocket in a ligand-bound state, these compounds might prevent caspase-3 from cleaving its targets, thereby reducing apoptosis. This aligns with the goal of nephroprotection: caspase inhibition has been shown to attenuate cisplatin-induced tubular cell apoptosis[17,40]. Among the docked ligands, BTDMP and HMPFP showed the highest binding energies to caspase-3 (both in the –8.5 to –9.0 kcal/mol range), correlating with the extensive hydrogen bonding and aromatic stacking they achieve in the active site. Still, this binding may be enough to impede caspase-3 activity partially.

NLRP3 inflammasome activation by oxidative stress signals triggers inflammatory cytokine release, further amplifying renal injury[12,40]. Fig. 5b, shows the interaction between the ligands and NLRP3 inflammasomes. Here the compounds were docked against NLRP3 NACHT domain (the nucleotide-binding domain responsible for oligomerization) especially the ATP-binding pocket of the NACHT domain. DHP forms multiple hydrogen bonds with key residues to the P-loop Lysine or sensor loop arginine that bind ATP. It also has hydrophobic contacts to His522, Ile234, Trp416, Leu413, showing only a weak edge-to-face interaction with Thr233. This combination of polar and non-polar interactions yields a very tight binding (–10.5 kcal/mol).

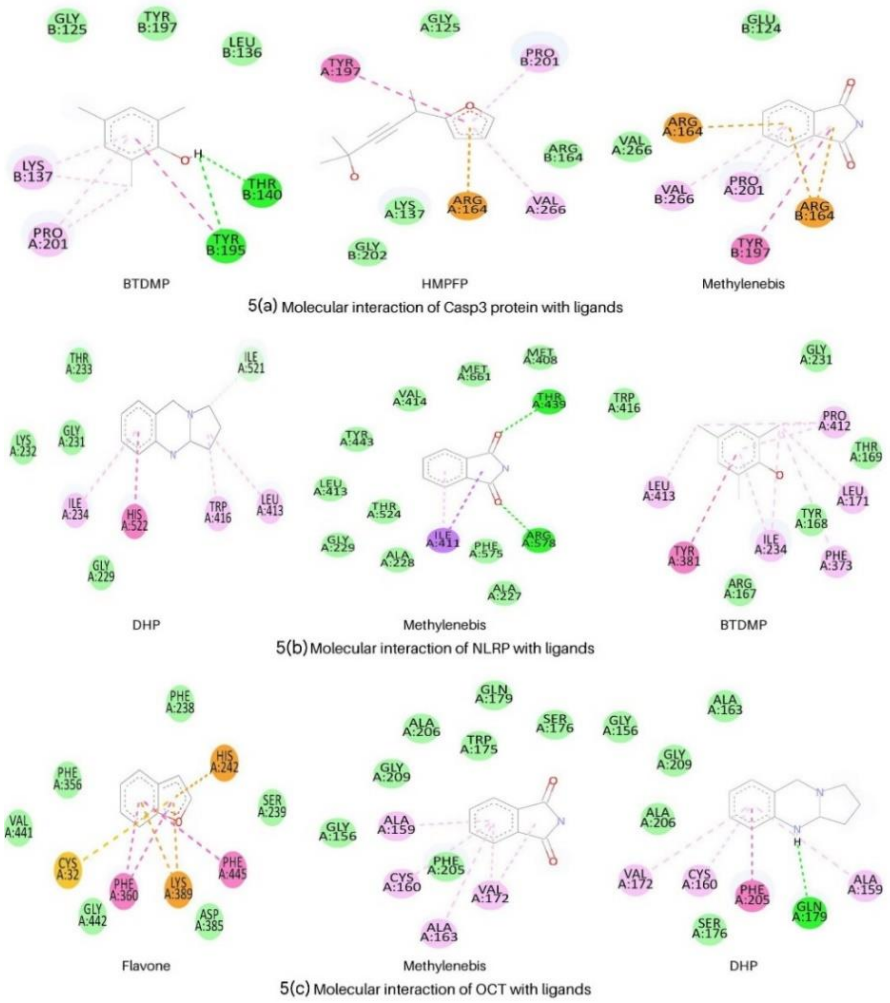

Figure 5: Molecular interactions of target proteins 5(a) Casp3, 5(b) NLRP and 5(c) OCT2 with top three interacting ligands

Methylenebis uniquely delivers dual H-bonds to Thr439 and Arg578, supplemented by hydrophobic packing against Ile411 and Phe575 in this protein. The dual polar latch plus hydrophobic filling in Methylenebis most closely parallels known NACHT-locking inhibitors, implying superior potential to immobilise the ATP-binding clutch and curb inflammasome assembly. BTDMP spreads over both hydrophobic (Leu171, Phe373, Ile234) and aromatic (Tyr381) side chains, but lacks direct polar anchors. These docking results suggest that ligands could suppress NLRP3 activation, reducing IL-1β-mediated inflammation. In our current study, the ligands DHP, Methylenebis and BTDMP demonstrated strong biding affinities ranging from -10.5 to -9.5 kcal/mol to the NLRP3 protein, suggesting their potential to inhibit its activation by binding to the active site.

Dehydroisohispanolone (DIH) binds covalently to the ATP binding site of NLRP3, effectively inhibiting the inflammasome[9]. Together, these findings provide compelling evidence that the identified plant ligands may serve as potent NLRP3 inhibitors with anti-inflammatory potential. The organic cation transporter-2 (OCT2) is a trans membrane transporter and the docking was performed in a homology model of its central cavity (substrate translocation pore). The cisplatin uptake is transporter-mediated, primarily via OCT2, accentuates intracellular platinum accumulation, intensifying nephrotoxic outcomes[3,14]. Fig. 5 (c) indicates that the ligands bind within the aqueous cavity, interacting with both polar and hydrophobic residues lining the channel.

The central aqueous cavity presents an inner ring of hydrophobes made by the amino acid residues Phe205, Val172, Ala159/163, Cys160 and bracketed by polar gatekeepers Gln179 and Ser176. Flavone exploits mixed binding: π-stacking with Phe238 and Phe445, hydrophobic anchoring to Phe360; Phe356 and electrostatic links to His242, Lys389, Cys32 that orient the polycyclic core toward the pore axis. Methylenebis by its hydrophobic nature clamps the Val172, Ala159/163, producing the sparsest contact array. Any of the three could sterically hinder cisplatin passage. DHP keeps the hydrophobic triad (Phe205, Cys160, Val172) and introduces a single hydrogen bond to Gln 179, positioning its ring plane across the conduit. The key point is that these compounds could occupy the transporter's substrate site, potentially blocking cisplatin

uptake. We observed that flavone emerged as a promising compound in our study exhibiting a strong binding affinity of -10.3 kcal/mol toward OCT2, indicating its potential as an effective inhibitor. A group of flavonoids significantly reduced cisplatin-induced cyto-toxicity and improved renal function by lowering urea and creatinine levels. Their pharmacophore model emphasized the importance of aromatic rings and hydrogen bonding in OCT2 inhibition[30]. Collectively, these highlight flavonoids, as potential agents to mitigate OCT2-mediated cisplatin nephrotoxicity by curbing its entry into the renal cells.

Thus, the combined therapeutic strategy represented by these bioactive compounds from *Boerhavia diffusa* not only offers a rational basis for nephroprotective therapy but also addresses the complexity of cisplatin nephrotoxicity more comprehensively than conventional monotherapies. The identified ligands' binding affinity and specificity must be substantiated by targeted *in vitro* cell culture models, followed by *in vivo* animal studies to ascertain their pharmacokinetic behavior, therapeutic efficacy and overall safety. Despite these limitations, the implications of the current findings are significant.

By pinpointing bioactive metabolites of *B. diffusa* and their molecular targets, this research provides a scientifically robust rationale for developing plant-based therapies to combat drug-induced nephrotoxicity. The multi-target mode of action revealed herein may lead to superior nephroprotective strategies compared to current single-target approaches, offering comprehensive renal protection in patients undergoing nephrotoxic drug therapies. Ultimately, the outcomes of this study serve as a vital preliminary foundation, guiding future experimental investigations toward innovative, safer and more effective renal protective therapeutics derived from natural sources.

Conclusion

This study provides a mechanistic framework for the nephroprotective reputation of *Boerhavia diffusa*. Chloroform and ethanol extracts furnished chemically diverse metabolites that after ADME prioritisation, were shown by network pharmacology to converge on six high-value cisplatin-toxicity nodes. Docking results spotlight three scaffolds with sub-micromolar, multi-target affinities: DHP – dual AKT1/NLRP3 blocker predicted to relieve mTOR-inhibited autophagy while dampening IL-1β/IL-18-mediated inflammation. HMPFP – potent AKT1 is hinge binder that simultaneously antagonises NLRP3 and OCT suggesting combined autophagic, anti-pyroptotic and uricosuric benefits. BTDMP– bisphenolic is bridge locking AKT1 in an inactive conformation, forestalling inflammasome assembly and occluding renal transport pores.

All three satisfy contemporary drug-likeness rules, lack PAINS alerts and display homogeneous strong docking across AKT1, NLRP3 and OCT, aligning with the systems-biology effective view. While *in silico* predictions require biochemical and *in vivo* corroboration, the present multi-omics workflow (GC-MS→ADME→PPI/GO→docking) offers a scalable template for mining other ethno medicines. These findings provide a mechanistic rationale for the empirically observed Reno protective effects of *Boerhavia diffusa* in cisplatin therapy and pave the way for further validation *in vitro* and *in vivo*.

References

1. Biswas P., Mathur D., Jinal Dinesh, Hitesh Kumar Dinesh and Manjunath B., Computational Analysis using Multi-ligand Simultaneous Docking of Withaferin A and Garcinol Reveals Enhanced BCL-2 and AKT-1 Inhibition, 2025 International Conference on Innovation in Computing and Engineering (ICE), Greater Noida, India, 1–6 **(2025)**

2. Borse P.V., Patil L.B., Patil J.N., More J., Suryawanshi C., Sinhal A.P. and Jadhav N., A comprehensive exploration of Punarnava's (Boerhavia diffusa) ethnomedicinal, therapeutic and traditional applications, *World J. Pharm. Pharm. Sci*., **12(11)**, 925–951 **(2023)**

3. Ciarimboli G., Ludwig T., Lang D., Pavenstädt H., Koepsell H., Piechota H.J., Haier J., Jaehde U., Zisowsky J. and Schlatter E., Cisplatin nephrotoxicity is critically mediated via the human organic cation transporter 2, *Am. J. Pathol*., **167(6)**, 1477–1484 **(2005)**

4. Daina A., Michielin O. and Zoete V., SwissADME: a free web tool to evaluate pharmacokinetics, drug-likeness and medicinal chemistry friendliness of small molecules, *Sci. Rep*., **7(1)**, 42717 **(2017)**

5. Dallakyan S. and Olson A.J., Small-molecule library screening by docking with PyRx, In Chem. Biol.: Methods Protocols, 243–250 **(2014)**

6. Fang C.Y., Lou D.Y., Zhou L.Q., Wang J.C., Yang B., He Q.J., Wang J.J. and Weng Q.J., Natural products: potential treatments for cisplatin-induced nephrotoxicity, *Acta Pharmacol. Sin*., **42(12)**, 1951–1969 **(2021)**

7. Franke R.M., Kosloske A.M., Lancaster C.S., Filipski K.K., Hu C., Zolk O., Mathijssen R.H. and Sparreboom A., Influence of Oct1/Oct2-deficiency on cisplatin-induced changes in urinary N-acetyl-β-D-glucosaminidase, *Clin. Cancer Res*., **16(16)**, 4198–4206 **(2010)**

8. Ge S.X., Jung D. and Yao R., ShinyGO: a graphical gene-set enrichment tool for animals and plants, *Bioinformatics*, **36(8)**, 2628–2629 **(2020)**

9. González-Cofrade L., Cuadrado I., Ángel Amesty, Estévez-Braun A., Beatriz and Sonsoles Hortelano, Dehydroisohispanolone as a Promising NLRP3 Inhibitor Agent: Bioevaluation and Molecular Docking, *Pharmaceuticals*, **15(7)**, 825–825 **(2022)**

10. Huang G., Zhang Y., Zhang Y., Zhou X., Xu Y., Wei H., Chen X. and Ma Y., Oridonin attenuates diabetes induced renal fibrosis via the inhibition of TXNIP/NLRP3 and NF κB pathways by activating PPARγ in rats, *Exp. Clin. Endocrinol. Diabetes*, **132(10)**, 536–544 **(2024)**

11. Jin X., An C., Jiao B., Safirstein R.L. and Wang Y., AMP-activated protein kinase contributes to cisplatin-induced renal epithelial cell apoptosis and acute kidney injury, *American Journal of Physiology-Renal Physiology*, **319(6)**, F1073-80 **(2020)**

12. Jin X., An C., Jiao B., Safirstein R.L. and Wang Y., AMP-activated protein kinase contributes to cisplatin-induced renal epithelial cell apoptosis and acute kidney injury, *Am. J. Physiol.-Renal Physiol*., **319(6)**, F1073–F1080 **(2020)**

13. Ju S.M., Bae J.S. and Jeon B.H., AMP-activated protein kinase contributes to ROS-mediated p53 activation in cisplatin-induced nephrotoxicity, *Eur. Rev. Med. Pharmacol. Sci.,* **25(21)**, 6691–6700 **(2021)**

14. Łapczuk-Romańska J., Droździk M., Oswald S. and Droździk M., Kidney drug transporters in pharmacotherapy, *Int. J. Mol. Sci.*, **24(3)**, 2856 **(2023)**

15. Li Q., Huang Z., Liu D., Zheng J., Xie J., Chen J., Zeng H., Su Z. and Li Y., Effect of berberine on hyperuricemia and kidney injury: a network pharmacology analysis and experimental validation in a mouse model, *Drug Design, Development and Therapy*, **15**, 3241-54 **(2021)**

16. Liu X., SLC family transporters, In: Drug Transporters in Drug Disposition, Effects and Toxicity, 101–202 **(2019)**

17. McSweeney K.R., Gadanec L.K., Qaradakhi T., Ali B.A., Zulli A. and Apostolopoulos V., Mechanisms of cisplatin-induced acute kidney injury: pathological mechanisms, pharmacological interventions and genetic mitigations, *Cancers*, **13(7)**, 1572 **(2021)**

18. Niu X., Xu C., Cheuk Y.C., Xu X., Liang L., Zhang P. and Rong R., Characterizing hub biomarkers for post-transplant renal fibrosis and unveiling their immunological functions through RNA sequencing and advanced machine learning techniques, *J. Transl. Med.*, **22(1)**, 186 **(2024)**

19. Pandey A.K. and Loscalzo J., Network medicine: An approach to complex kidney disease phenotypes, *Nat. Rev. Nephrol.*, **19(7)**, 463–475 **(2023)**

20. Paolini E., Quattrini L., Coviello V., Antonioli L., Fornai M., Blandizzi C., Keun Oh W. and La Motta C., Isoindoline Derivatives for Use as Ampk Activators, Available at: https://patents.google.com/patent/WO2018189679A1/en **(2018)**

21. Peres L.A. and Cunha Júnior A.D., Acute nephrotoxicity of cisplatin: molecular mechanisms, *Braz. J. Nephrol*., **35**, 332–340 **(2013)**

22. Qi J., Xue Q., Kuang L., Xie L., Luo R. and Nie X., Berberine alleviates cisplatin-induced acute kidney injury by regulating mitophagy via PINK 1/Parkin pathway, *Translational Andrology and Urology*, **9(4)**, 1712 **(2020)**

23. Sasidharan S., Chen Y., Saravanan D., Sundram K.M. and Latha L.Y., Extraction, isolation and characterization of bioactive compounds from plants' extracts, *Afr. J. Tradit. Complement, Altern. Med.*, **8(1)**, 1-10 **(2011)**

24. Sharma V., Gupta A., Singh M., Singh A., Chaudhary A.A., Ahmed Z.H., Khan S., Rustagi S., Kumar S. and Kumar S., Phytochemical baicalin potentially inhibits Bcl-2 and VEGF: an *in silico* approach, *Frontiers in Bioinformatics*, **5**, https://doi.org/10.3389/fbinf.2025.1545353 **(2025)**

25. Singh H., Singh T., Buttar H.S., Kaur S., Arora S., Télessy I.G. and Singh B., The pathophysiology of liver disorders and pharmacotherapy options with special reference to traditional herbal medicines: A comprehensive review, Biomed. Transl. Res.: Drug Des. Disc., 549–583 **(2022)**

26. Son A., Park J., Kim W., Yoon Y., Lee S., Ji J. and Kim H., Recent advances in omics, computational models and advanced screening methods for drug safety and efficacy, *Toxics*, **12(11)**, 822 **(2024)**

27. Song Z., Zhu J., Wei Q., Dong G. and Dong Z., Canagliflozin reduces cisplatin uptake and activates Akt to protect against cisplatin-induced nephrotoxicity, *Am. J. Physiol.-Renal Physiol.*, **318(4)**, F1041–F1052 **(2020)**

28. Su H., Wan C., Song A., Qiu Y., Xiong W. and Zhang C., Oxidative stress and renal fibrosis: mechanisms and therapies, *Renal Fibrosis: Mechanisms and Therapies*, **1165**, 585–604 **(2019)**

29. Szklarczyk D., Gable A.L., Nastou K.C., Lyon D., Kirsch R., Pyysalo S., Doncheva N.T., Legeay M., Fang T., Bork P. and Jensen L.J., The STRING database in 2021: customizable protein–protein networks and functional characterization of user-uploaded gene/measurement sets, *Nucleic Acids Res.*, **49(D1)**, D605–D612 **(2021)**

30. Tan H., Wang F., Hu J., Duan X., Bai W., Wang X., Wang B., Su Y. and Hu J., Inhibitory interaction of flavonoids with organic cation transporter 2 and their structure–activity relationships for predicting nephroprotective effects, *Journal of Applied Toxicology*, **43(10)**, 142 **(2023)**

31. Tang C., Livingston M.J., Safirstein R. and Dong Z., Cisplatin nephrotoxicity: new insights and therapeutic implications, *Nat. Rev. Nephrol*., **19(1)**, 53–72 **(2023)**

32. Tangeda V., Lo Y.K., Babuharisankar A.P., Chou H.Y., Kuo C.L., Kao Y.H., Lee A.Y. and Chang J.Y., Lon upregulation contributes to cisplatin resistance by triggering NCLX-mediated mitochondrial Ca^{2+} release in cancer cells, *Cell Death Dis.*, **13(3)**, 241 **(2022)**

33. Thomadaki H. and Scorilas A., BCL2Family of Apoptosis-Related Genes: Functions and Clinical Implications in Cancer, *Critical Reviews in Clinical Laboratory Sciences*, **43(1)**, 1–67 **(2006)**

34. Tiwari P., Soni N., Wal P. and Srivastava M., A review of Punarnava's pharmacological profile focusing on its beneficial and adverse effects, *Curr. Tradit. Med*., **9(5)**, 61–70 **(2023)**

35. Vilaysane A., Chun J., Seamone M.E., Wang W., Chin R., Hirota S., Li Y., Clark S.A., Tschopp J., Trpkov K. and Hemmelgarn B.R., The NLRP3 inflammasome promotes renal inflammation and contributes to CKD, *J. Am. Soc. Nephrol.*, **21(10)**, 1732–1744 **(2010)**

36. Volarevic V., Djokovic B., Jankovic M.G., Harrell C.R., Fellabaum C., Djonov V. and Arsenijevic N., Molecular mechanisms of cisplatin-induced nephrotoxicity: a balance on the

knife edge between renoprotection and tumor toxicity, *J. Biomed. Sci.*, **26**, 1–4 **(2019)**

37. Wu H. and Huang J., Drug-induced nephrotoxicity: pathogenic mechanisms, biomarkers and prevention strategies, *Curr. Drug Metab.*, **19(7)**, 559–567 **(2018)**

38. Xiang H., Zhu F., Xu Z. and Xiong J., Role of inflammasomes in kidney diseases via both canonical and non-canonical pathways, *Front. Cell Dev. Biol*., **8**, 106 **(2020)**

39. Zhang H., Dong Q.Q., Shu H.P., Tu Y.C., Liao Q.Q. and Yao L.J., Mechanistic insights into the renoprotective role of curcumin in cisplatin-induced acute kidney injury: network pharmacology analysis and experimental validation, *Bioengineered*, **12(2)**, 11039-54 **(2021)**

40. Zhou Z. and Li Q., The role of pyroptosis in the pathogenesis of kidney diseases, *Kidney Diseases*, **9(6)**, 443-58 **(2023)**.

(Received 11th August 2025, accepted 08th September 2025)